A&A 402, L27–L34 (2003)
DOI: 10.1051/0004-6361:20030335

Astronomy & Astrophysics

The Odin satellite⋆

I. Radiometer design and test

U. Frisk[1], M. Hagström[2], J. Ala-Laurinaho[3], S. Andersson[4], J.-C. Berges[5], J.-P. Chabaud[6,17], M. Dahlgren[2], A. Emrich[4], H.-G. Florén[7], G. Florin[1], M. Fredrixon[2], T. Gaier[8], R. Haas[9], T. Hirvonen[3], Å. Hjalmarsson[2], B. Jakobsson[1], P. Jukkala[10], P. S. Kildal[11], E. Kollberg[11], J. Lassing[11], A. Lecacheux[12], P. Lehikoinen[3], A. Lehto[3], J. Mallat[3], C. Marty[6], D. Michet[12], J. Narbonne[6], M. Nexon[6], M. Olberg[2], A. O. H. Olofsson[2], G. Olofsson[7], A. Origné[5], M. Petersson[13], P. Piironen[3], R. Pons[6], D. Pouliquen[5], I. Ristorcelli[6], C. Rosolen[12], G. Rouaix[6], A. V. Räisänen[3], G. Serra[6,17], F. Sjöberg[1], L. Stenmark[14], S. Torchinsky[15], J. Tuovinen[3], C. Ullberg[14], E. Vinterhav[1], N. Wadefalk[11], H. Zirath[11], P. Zimmermann[16], and R. Zimmermann[16]

[1] Swedish Space Corporation, Box 4207, 171 04 Solna, Sweden
[2] Onsala Space Observatory, Chalmers University of Technology, 439 92 Onsala, Sweden
[3] Helsinki University of Technology, Radio Laboratory, PO Box 3000, 02015 HUT, Espoo, Finland
[4] Omnisys Instruments, Gruvgatan 8, 421 30 Gothenburg, Sweden
[5] Observatoire Astronomique Marseille Provence, LAM, CNRS, Traverse du Siphon, BP 8, 13376 Marseille Cedex 12, France
[6] Centre d'Étude Spatiale des Rayonnements, CNRS, 9 avenue du Colonel Roche, 31028 Toulouse, France
[7] Stockholm Observatory, SCFAB, Roslagstullsbacklen 21, 106 91 Stockholm, Sweden
[8] Jet Propulsion Laboratory, 4800 Oak Grove Drive, Pasadena, California 91109, USA
[9] TRW, M5/2154, 1 Space Park, Redondo Beach, CA 90278, USA
[10] Ylinen Electronics Ltd, Teollisuustie 9 A, 02700 Kauniainen, Finland
[11] Chalmers University of Technology, 412 96 Gothenburg, Sweden
[12] Observatoire de Paris, Département ARPEGES, 92195 Meudon Principal Cedex, France
[13] Saab Ericsson Space, 405 15 Gothenburg, Sweden
[14] ACR, Redskapsvägen 7, 619 00 Trosa, Sweden
[15] Canadian Space Agency, PO Box 7275, Ottawa, Ontario K1L 8E3, Canada
[16] Radiometer Physics, Birkenmaarstrasse 15, 5309 Meckenheim, Germany
[17] We regret the deaths of Guy Serra in 2000 and of Jean-Paul Chabaud in 2001

Received 6 December 2002 / Accepted 2 March 2003

Abstract. The Sub-millimetre and Millimetre Radiometer (SMR) is the main instrument on the Swedish, Canadian, Finnish and French spacecraft Odin. It consists of a 1.1 metre diameter telescope with four tuneable heterodyne receivers covering the ranges 486−504 GHz and 541−581 GHz, and one fixed at 118.75 GHz together with backends that provide spectral resolution from 150 kHz to 1 MHz. This Letter describes the Odin radiometer, its operation and performance with the data processing and calibration described in Paper II.

Key words. space vehicles – space vehicles: instruments – telescopes – techniques: spectroscopic

1. Introduction

The atmosphere limits ground-based observations and makes it impossible for frequencies close to strong water and oxygen lines to reach the ground. The Odin radiometer was to a large extent designed to fill in these gaps regarding what was then understood to be the major cooling lines of molecular clouds. It was optimised for observations of spectral lines in the sub-mm region from the oxygen isotopes of ortho-H_2O ($1_{10} - 1_{01}$) and of O_2 ($3_2 - 1_2$) together with the mm line O_2 ($1_1 - 1_0$). The inclusion of the 118.75 GHz transition is very important since it improves the sensitivity to detect oxygen by more than an order of magnitude (Pagani et al. 2003). To aid the interpretation of water measurements also the ground state transition of ortho-NH_3 ($1_0 - 0_0$) was made a priority. Since the instrument

Send offprint requests to: U. Frisk, e-mail: urban.frisk@ssc.se

⋆ Odin is a Swedish-led satellite project funded jointly by the Swedish National Space Board (SNSB), the Canadian Space Agency (CSA), the National Technology Agency of Finland (Tekes) and Centre National d'Études Spatiales (CNES). The Swedish Space Corporation was the prime contractor, and is also responsible for the satellite operation.

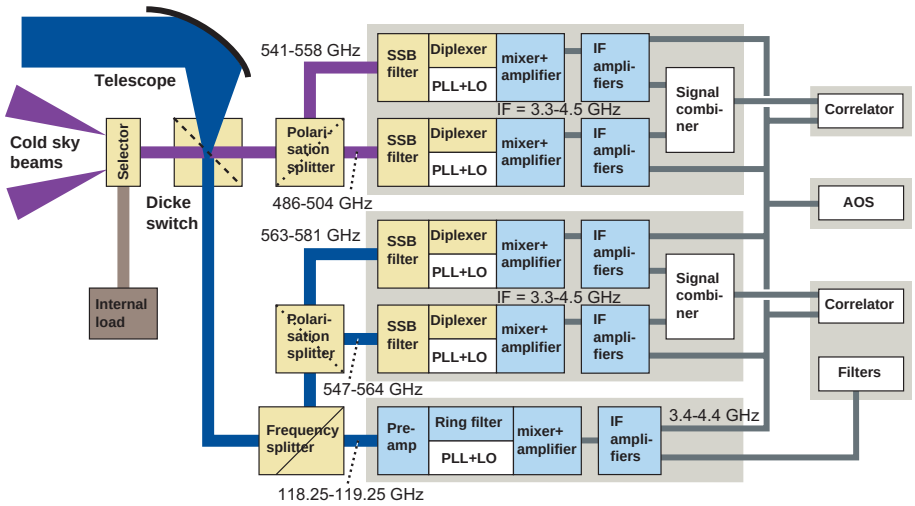

Fig. 1. This block diagram shows the layout of the instrument. High frequency signals from the telescope and the signal references are fed via pre-optics such as the Dicke switch, the single sideband filters and the diplexers for local oscillator injection, to the mixers. The mixers together with the first low noise amplifiers are mounted inside a cryostat. IF signals are after further amplification routed to the backend spectrometers.

is used by aeronomers to observe the Earth atmosphere its design also had to meet their needs. Thus, for instance the final frequency coverage (cf. Hjalmarsson et al. 2003) represents a compromise between both communities. Sensitive measurements of the amount of water is an objective which is shared and in this case the same transition is used for both astronomical targets and for Earth's atmosphere. The primary driver for the astronomical observations has been sensitivity while suppression of unwanted antenna lobes and receiver sidebands are more important for the atmospheric observations. Sometimes the optimum design for astronomy and aeronomy is not the same, but overall the combined mission has led to a superior performance of the instrument. Since heterodyne receivers for these frequencies had not flown in space before, their short and long term behaviour was uncertain. In addition, the abundance of both water and oxygen was unknown. Hence the radiometer was designed for maximum flexibility making it possible to adapt the instrument to changing scientific requirements. This gives added capability to handle failure or degradation of parts of the receivers. Wide frequency coverage was selected to be able to tune to other species, carry out frequency scans and to reach red-shifted galaxies.

We describe below the design of the instrument, test, alignment and in-orbit operation. Although similar instruments are now common on the ground, the very limited power available in a small spacecraft forced new designs optimised for low power consumption. The need to withstand the launch and in-orbit environment added further constraints.

The second part of this article is about the calibration and data processing of the instrument data, see Olberg et al. (2003).

2. The instrument design

2.1. General properties

The receivers are arranged as five independent signal chains in two groups that are time multiplexed by a switching mirror (Dicke switch) such that one group is receiving the signal from the telescope as the other receives a reference or calibration signal. Figure 1 shows the radiometer layout and also the separation of frequencies, the ground state water lines have been included in both groups for redundancy reasons and to permit improved observing efficiency. Within each group the signals are further split according to polarisation. This arrangement avoids complete loss of all the receivers from a hypothetical mechanical failure of the Dicke switch. The mechanism operates every 1 to 10 s with the backends generating one spectrum per position. It is also possible to use position switching with the complete spacecraft and the Dicke switch halted. The backend spectrometers monitor attitude control information to blank out bad data during attitude changes. The sub-mm receivers select sideband and inject the LO signal using polarising interferometers while the mm receiver uses a fixed tuned ring filter. The Schottky mixers, the mm preamplifier with ring filter, and the low noise amplifiers (LNA) are cooled and mounted inside the cryostat. The 1.2 GHz wide intermediate frequency (IF) signals are amplified and sent in parallel to one acousto-optical (AOS) and two autocorrelation spectrometers. Basic data are shown in Tables 1 and 2.

Table 1. Radiometer summary.

Antenna	1.1 m offset Gregorian
Pointing accuracy	10″
Pointing stability	4″ per hour
Frequency range	118.75, 486-504, 541-581 GHz
Typical system noise	600, 3300, 3300 K
Spectral resolution	125 to 1000 kHz
Backend bandwidth	100 to 1000 MHz
Cooling	Stirling cycle to 140 K

Table 2. Telescope parameters.

Frequency [GHz]	119	480	540	580
Beam size [arc min]	9.96	2.42	2.20	2.05
Aperture efficiency	0.72	0.70	0.69	0.69
Main beam efficiency	0.91	0.89	0.89	0.89

2.2. Telescope and optical components

Odin has a dual reflector offset Gregorian telescope with shaped surfaces designed by Moldsvor et al. (1994) in order to combine low side lobe levels with high gain. The reflectors have been manufactured from carbon-fibre-reinforced-plastics (CFRP) face sheets on CFRP honeycomb with the front surfaces coated with vacuum deposited aluminium. These have a measured accuracy of 8 μm rms for the primary and 5 μm rms for the secondary. The support structure (cf. Sjöberg 1996) is a single structure in CFRP that in addition integrates support for the star tracker optical heads, see Fig. 2. By coupling the star tracker optics to the telescope structure, the effect of thermoplastic deformations on telescope pointing is minimised. Instead of allowing the telescope to cool down in space, it is kept around room temperature simplifying the on-ground testing. Temperature is maintained by covering the back of the reflectors with multi-layer insulation (MLI) in combination with surface heaters.

The reflector surfaces, equipped with reference points, were first measured in a 3-d coordinate machine with micron accuracy. Then their optimum relative position was determined using physical optics calculations. The reference points were later used during the telescope integration, in a photogrammetric method to align the reflectors to a relative accuracy of about 50 μm. Using the measured shape of the reflector surfaces the aperture and main beam efficiencies and beam size have been calculated, see Table 2. These values include an expected loss of efficiency of −0.3 dB due to non-perfect alignment.

The reference switch and calibration mechanisms are based on redundant drive stepper motors with the switch mirror made out of aluminised Mylar film to reduce mass. The time to switch between positions is less than 125 ms and the integration time can be set in the range 1 to 10 s. The two sky beams are offset more than 40° from the telescope axis with a half power beam width (HPBW) of 4.7° at 119 GHz and 4.5° in the submm range.

Tuneable, polarising Martin-Pupplet interferometers are used for single sideband (SSB) filtering and local oscillator injection. The filters can be tuned independently to optimise the choice of frequency for maximum suppression. Their mechanisms have loudspeaker type actuators that move a rooftop mirror mounted on an axis suspended by disk springs. The position is servo-controlled with redundant drive motors using inductive position sensors mounted such that they are compensated for thermal changes. Figure 3 shows the assembled diplexer unit. The unwanted sideband has a measured maximum suppression of 35 dB falling to 19 dB at the edge of the IF band and is coupled to an ambient temperature load. The 119 GHz mixer is fix-tuned to suppress the sideband, not using pre-optics.

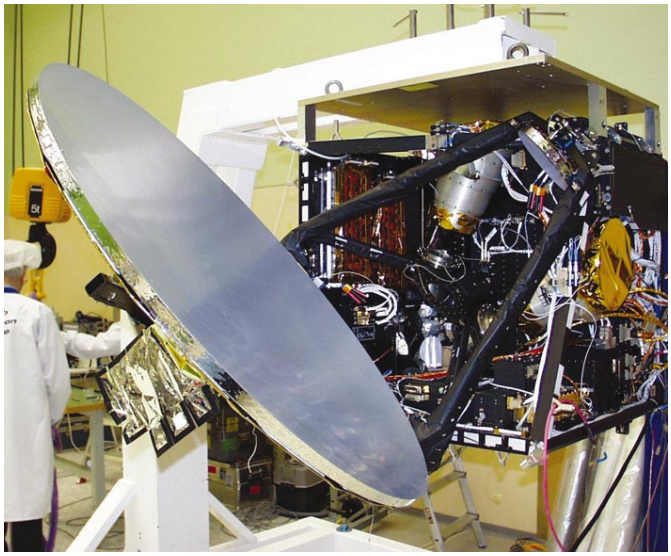

Fig. 2. The Odin CFRP main reflector with sub reflector can be seen mounted on the CFRP support structure that also holds the star tracker optical heads. Star tracker baffles are attached to the spacecraft structure. The radiometer platform is horizontal on this photo.

The internal optics in the radiometer consists of elliptical mirrors, corner cube reflectors and grids. The mirrors used in the radiometer have been precision turned in aluminium and equipped with alignment pins for very accurate mounting. A dichroic plate separates the mm signal from the sub-mm and via a lens-mirror combination feeds the signal into the Potter horn attached to the mm amplifier. Calibration is made using an internal ambient temperature load at around 300 K made out of carbon loaded polyethylene tiles optimised for 500 GHz reflecting less than −30 dB. This material is also used for the SSB terminations. The temperature of the material is known better than 0.2 K using redundant integrated temperature sensors. The calibration tiles form a cavity to improve the performance at 119 GHz where otherwise the reflections would be −20 dB.

2.3. Frequency down-conversion and amplification

The mm receiver is equipped with a three-stage InP based preamplifier to improve its sensitivity. The incoming radiation is fed into a waveguide with coupling to the MMIC amplifier via waveguide mounted probes. Pre-launch laboratory measurements showed that with a physical temperature of 120 K the amplifier had a noise temperature of 280 K and a gain of 13 dB.

Fixed-tuned mixers consisting of waveguide mounted Schottky diodes are used to down-convert the signals. The mm mixer design by Lehikoinen et al. (1996) is using a planar diode while the sub-mm mixers are whisker contacted. All mixers are open ended and have a conversion loss of about 7 dB. The 3.9 GHz intermediate frequency (IF) signals are amplified by cryogenic two stage GaAs HEMT amplifiers providing about 30 dB amplification. The typical amplifier noise is better

than 30 K, including the circulator placed between the mixer and the amplifier. The warm IF section provides 30 dB further amplification, splits the signal into four and feeds the three backends. The fourth path is used to combine two sub-mm 400 MHz IF bands and route to each of the two autocorrelators. This way signals from more frontends can be processed simultaneously than was originally planned.

Local oscillator (LO) power is generated from mechanically fixed-tuned solid-state Gunn oscillators. In the sub-mm range the frequency multiplied LO signal can be electrically tuned over 8 GHz and is transmitted via a Potter horn into a diplexer designed like the SSB filter described above. Part of the LO power is coupled into a harmonic mixer before going into the frequency doubler followed by a tripler. A tuned YIG source is used as harmonic oscillator and is locked to a 10 MHz reference with a stability of 5×10^{-8}. The phase lock loop (PLL) (Emrich 1996) operates on the Varactor voltage while maintaining a constant voltage for the Gunn diode. In order to sufficiently suppress the Gunn phase noise, the PLL has a 3 MHz loop bandwidth. The mm receiver LO has fixed redundant 114.8 GHz oscillators that have their output transmitted by a gold coated stainless steel waveguide into the cryostat and injected via a temperature compensated ring filter described by Piironen et al. (1998). A fraction of the signal is harmonically mixed down to 50 MHz with 8.2 GHz dielectric resonance oscillators. Both are locked to a 100 MHz crystal reference with low phase noise. The synthesiser can be operated either giving a fixed frequency or hopping between two frequencies with a 100 MHz separation (114.75 GHz and 114.85 GHz). Biasing of the sub-mm mixers, amplifiers, multipliers and Gunn sources are controlled by two PLL control units. These units act as the front-end controllers and also monitor voltages, currents and temperatures. They also control the phase lock loop electronics for the sub-mm local oscillators. The electronics have been distributed in separate boxes to reduce interference.

2.4. Cryostat with cooling

The cryostat houses the low temperature sections of the mm- and sub-mm receivers at around 140 K for the mixers/preamplifiers and 160 K for the low noise IF amplifiers. The sub-mm mixers together with the coupling mirrors are mounted inside as is the mm horn attached to the InP pre-amplifier. The signals enter via apertures equipped with baffles for thermal protection with the sub-mm signals split according to polarisation by grids before the mixer horns. Stainless steel is used to reduce the conduction of heat via the waveguide and the IF semi-rigid cables. The inside of the cryostat is suspended by Kevlar strings and protected by about 30 layers of multi-layer insulation.

Odin makes use of a single 50–80 K closed cycle Stirling cooler suspended by springs to reduce platform vibrations. This system was clamped during launch and later released in orbit. The cooler failed during start up in orbit probably due to stiction of the displacer piston. Eventually it was possible to get the cooler operating by heating the units near the allowed upper temperature limit and running it at maximum power. Once cool down started the mechanical clearances increased and performance gradually approached normal. Although the telemetry from the cooler still indicate some remaining low level disturbances the performance is otherwise nominal.

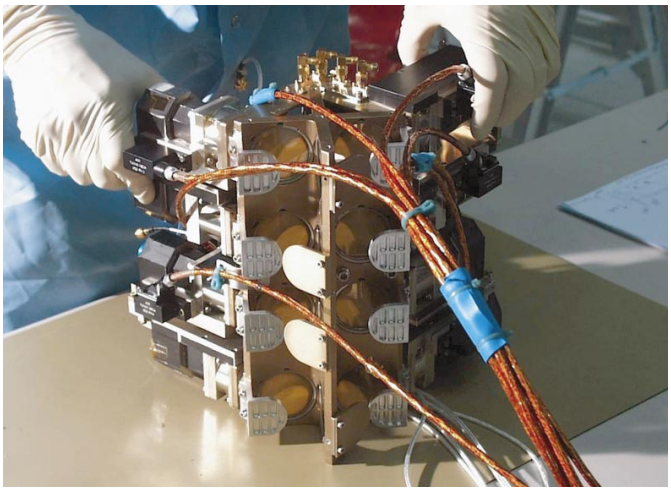

Fig. 3. The LO and diplexer unit with 4 sub-mm LO units, their drive electronics (out of view), 4 polarising Martin-Pupplet diplexers and 4 SSB filters. The 8 tuning mechanisms that adjust rooftop mirrors are seen sticking out on both sides. The mirrors of the fixed arms are to the front together with the backside of 2 SSB terminations.

2.5. Back-end spectrometers

The IF signals are passively split before routed to all backends, where input multiplexers are used to select receiver chain. In this way multiple backends can be connected to the same front-end for instance to combine high resolution in part of the IF band with wide bandwidth in low resolution. The Dicke switch and the attitude control system send status information on position and pointing error on the spacecraft synchronous data network that the spectrometers use to avoid integrating bad data. The acousto-optical spectrograph (AOS) (Lecacheux et al. 1996) relies on the modulation of laser light passing through a Bragg cell that after re-imaging forms a spectrum on an optical detector. In the Odin AOS (Lecacheux et al. 1998) the selected signal first goes to the IF processor that amplifies it by 40 dB, provides gain control, down-converts the frequency to 2.1 GHz and routes it to the acousto-optical processor. The IF signal modulates the Bragg cell and the spectrum is focussed on the 1728 pixel CCD via a Fourier lens and cylindrical optics. The temperature controlled laser diode is illuminating a Bragg cell via collimating optics and a beam expander. The spectrum is continuously read out and the data passed to the control unit. The unit has a −3 dB bandwidth of 1 GHz centred at 2.1 GHz and a frequency resolution of 1 MHz. The amplitude stability is better than 100 s judging from Allan variance tests. The control and power unit provides digital processing and controls the laser diode, temperatures and IF gain attenuation. It also interfaces to spacecraft power and control and telemetry. Temperature regulation (0.01 °C) of the whole optical box and stabilisation of the laser diode current ensure accurate determination of spectral amplitude and frequency.

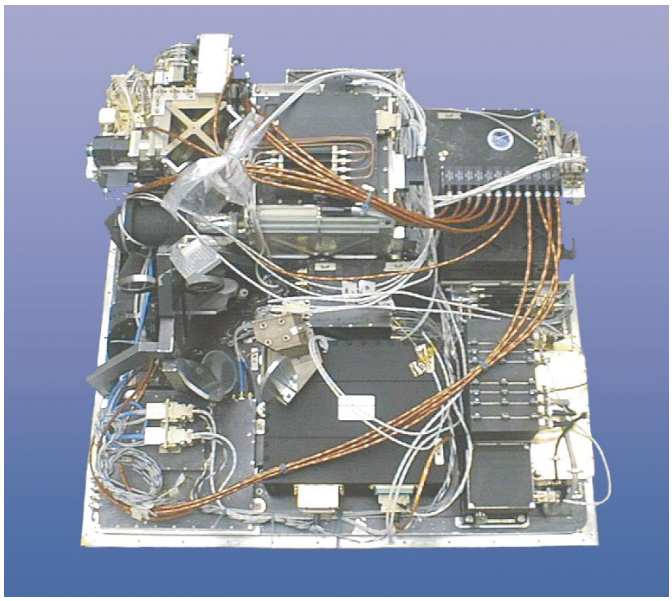

Fig. 4. The radiometer platform. From the front, on the left side is the autocorrelator with filterbank, pre-optics, Stirling cooler and LO structure. In the middle part is the cooler electronics with warm load, warm IF unit, PLL and control electronics, cryostat with biasing and, out of sight, the 119 GHz warm electronics. On the right is AOS, mechanism electronics and second autocorrelator.

The absolute frequency scale is checked once per orbit by an internal frequency comb generator.

The Odin autocorrelators (AC1 and AC2, Emrich 1997) is of hybrid type and filters the input signal by up to eight subbands before calculating the autocorrelation function of each band. The integrated spectrum is later retrieved via a Fourier transform in the data processing. The pre-filtering leads to reduced power consumption as it reduces the need for high speed processing. The eight single-sideband filters are organised in pairs by using upper and lower side-band of a common oscillator, thus forming four 200 MHz sub-bands. These can be individually placed within the 1.2 GHz input band. The maximum sum of the processed bandwidth (at 1 MHz resolution) is 800 MHz and the total number of channels is 768. The signals in each band are digitised by A/D converters and sent to the autocorrelator chips that integrate the autocorrelation function. The 96 lag chips are cascadable with internal time multiplexing and implements a 1.5 bit scheme. Thus, the spectrometer can be reconfigured to trade bandwidth to a highest resolution of 125 kHz. Data is read out and buffered by a transputer control processor. The measured power consumption of the total unit with 768 channels including IF processor, data processing, power and I/O interface is 12 W. The autocorrelator is using a chip set consisting of a custom designed digitiser and a correlator chip. The digitiser was made with a bipolar process and the correlator ASIC is a full custom design chip manufactured on a radiation tolerant 0.6 μ CMOS process. Special effort has been made to reduce power consumption of the chip to below 350 mW and to keep electrical noise very low.

3. Test and alignment

3.1. Telescope alignment with sub-mm methods

A test set-up was developed at CESR (Toulouse) to analyse the telescope image quality in the sub-mm range, with the objectives to find the telescope's best focus, optical axis and to control the alignment to, and image quality of, the receivers.

The tests were performed with a one meter diameter collimator operating both in the visible and sub-mm range (see Fig. 5) equipped with a motorised source system (high pressure mercury lamp + chopper). When used with a bolometer detector (4 K) in the telescope focal plane, the point spread function can be mapped without the receivers. The measurements were made in a large wavelength band $\Delta\lambda/\lambda \approx 25\%$ around $\lambda = 200\,\mu$m with a dynamic range of 30 dB from the diffraction peak. An analysis based on encircled energy plots determined the position of the best focus, and the corresponding best optical axis. The measured beam profile could be well reproduced by modelling the diffraction pattern. The focus was determined relative to the reference balls of the secondary mirror, by using a laser beam and a micrometer ruler. The optical axis direction was measured with theodolites from the incident collimated beam and referenced to cubic mirrors fixed on the reflectors structure. The resulting accuracy of this method was ±1.5 mm for the focal plane position and ±30″ for the best axis direction (cf. Ristorcelli et al. 2003). A similar method was used to control the focus and co-alignment of the radiometer channels to the telescope just before launch but after the system-level environmental tests. The Odin beam profiles have been measured for three receivers (495, 549 and 572 GHz) using both a broadband mercury lamp and Gunn Oscillator sources for the sub-mm bands (for the 119 GHz only with a Gunn source) in the focus of the collimator. Beam profiles were close to Gaussian down to the −5 dB level with a radius that was found close to the expected. The pointing directions of the receivers were measured with an accuracy of 2″ and all the sub-mm receivers showed alignment within 10″.

This set-up was also used to measure the OSIRIS (Murtagh et al. 2002) instrument optical axis with theodolites and adjust its pointing to that of the radiometer. OSIRIS is a near-IR imager, UV-visual wavelength spectrograph for atmospheric measurements.

3.2. Hologram test of telescope

The 119 GHz compact antenna test range (CATR) is based on a 2.4 m × 2.0 m hologram and was used to verify the antenna beam at 119 GHz. The setup was described by Ala-Laurinaho et al. (2001). Comparison between the theoretical and the measured quiet-zone fields of the hologram CATR demonstrated the correctness of the analysis method and also the importance of high quality physical joints between the hologram parts. The CATR was then used in the measurement of the 1.1-m offset reflector antenna on board the Odin spacecraft together with the 119 GHz receiver. The measured and calculated antenna radiation patterns were in good agreement in the main beam region confirming the expected telescope performance. The hologram

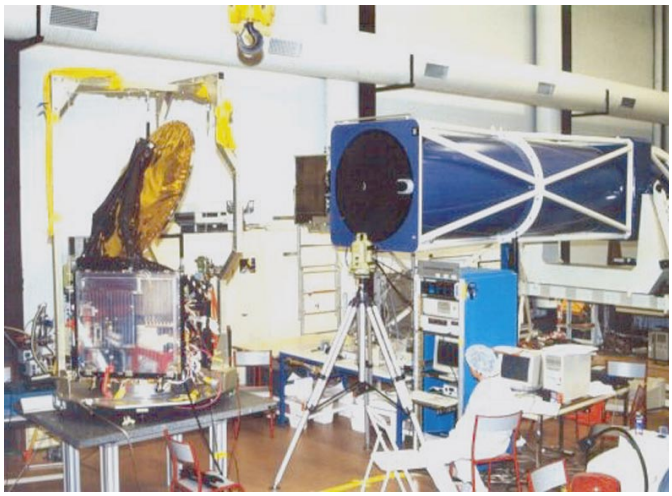

Fig. 5. The sub-mm collimator used for the alignment verification together with the Odin telescope with receiver platform during early tests. These were repeated after the launch simulation system tests just before launch.

tests were made before the final alignment of the receivers but demonstrated the internal alignment of the telescope itself.

3.3. Laboratory receiver tests

Pre-flight tests were carried out and the receivers were internally aligned before integration with the spacecraft and the telescope. The beams were scanned using an external moving source with the radiometer inside a vacuum chamber. Integrations up to 12 hours with the mechanical cooler operating were made to confirm that the cooler did not introduce disturbances and that the noise went down as the root of time. Before the cooler was mechanically isolated the cooler vibrations disturbed the tuning devices for the SSB and LO diplexer filters, causing them to oscillate. An external gas cell containing adjustable low-pressure water vapour was used to provide realistic signals.

Since the receivers are tuneable they can interfere in many different ways. For instance some frequency combinations cause the PLL not to find a proper lock. Extensive tests were made on the ground to confirm all pre-identified frequency combinations and over the expected range of Doppler velocities. Proper lock was verified and the level of the phase noise was recorded.

4. Operation of the radiometer

In order to facilitate independent development and testing by the different manufacturers involved, a radiometer control system based on self contained units with well defined interfaces was selected. Power and control was distributed such that failures would lead to a graceful degradation of performance. In addition, where possible, redundant designs have been used. There is no main controller for the instrument, instead the spacecraft main computer is used to instruct the various units that then stay synchronised using the on-board telemetry bus (cf. Lundin 2002). For instance the backend spectrometers use status information from both the attitude control computer and the chopper electronics to limit signal integration to periods with valid data.

The radiometer is set up for Dicke switched mode or position switching by configuring the switch mechanism together with the backend spectrometers and the attitude control system, see Fig. 1. Frequencies of the individual receivers are set by commanding the servo controlled diplexer tuning mechanisms and the PLL control units. Selecting receiver, frequency coverage, resolution and possibly integration time configures the backends.

The correlator bands are set to overlap in frequency to provide redundant data for adjusting the relative continuum levels. Frequency comb measurement and automatic gain search are made to ensure optimum performance. Doppler change resulting from spacecraft velocity is not compensated for during a measurement but in the ground processing. The maximum time allowed for an individual integration is thus limited to avoid degrading the spectral resolution due to differential Doppler shift.

Atmospheric spectra are recorded with an integration time of 2 s during the transit of the line of sight through the atmosphere. Together with spectra taken during the occultation, this data is used as a source for absolute frequency calibration and as a convenient confirmation that the radiometer is operating properly.

During the very extensive ground testing, procedures in Labview were used to automate the tests, evaluate results and to determine the fairly complex sequences to set the complete radiometer. The same software is also used to generate new in-orbit radiometer measurement modes or ones with a different Doppler velocity. These command sequences together with timing information and attitude control instructions are uploaded from ground and stored in the on-board mass memory as macros and later sent out by the spacecraft computer. The warm load calibration sequences and the atmospheric transitions are handled in the same manner.

The scheduling of astronomical targets are made in the pre-agreed time slots with a minimum length of one day maintaining a 50/50 split with the aeronomy community. The quite detailed time-line contains pointing information for the targets and instrument settings.

5. In-orbit performance

The system noise temperature is very stable but the gain varies with temperature during each orbit (Olberg et al. 2003). These variations are removed by the switching process and results in a highly stable signal with noise going down with time as expected, (Pagani et al. 2003). All the receivers have similar stability. The typical in-orbit SSB system noise temperature is 600 K at 119 GHz and around 3300 K in the sub-mm range.

To characterise the in-orbit telescope properties and pointing capability we have on many occasions simultaneously mapped the thermal emission of Jupiter at 492, 548 and 557 GHz. We find that the antenna beams at these frequencies are co-aligned to within 10″, a result very similar to pre-launch alignment result. Figure 7 displays a recent Jupiter map at 557 GHz – actually the combination of maps observed

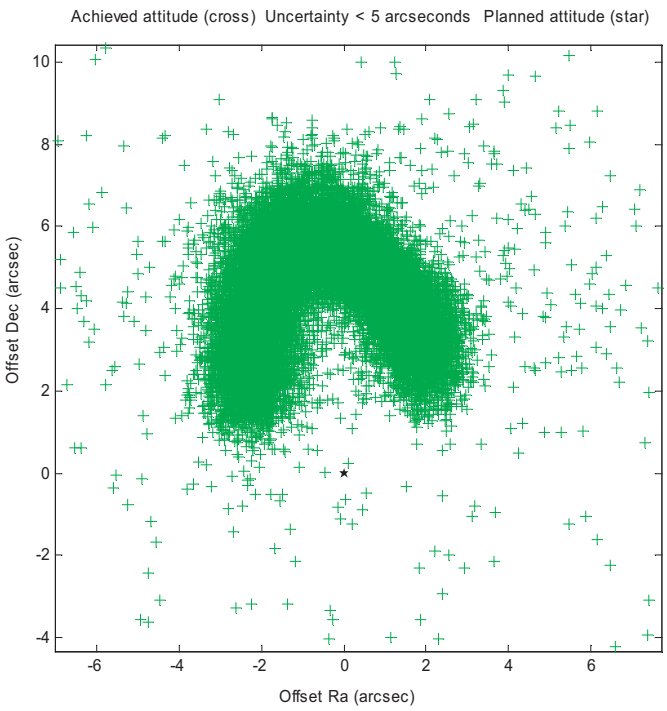

Fig. 6. Attitude error during several orbits. The position (0,0) is the target attitude. The points in this plot represent the attitude error at one sample (dt = 1 s), projected in declination and right ascension. The half circle results from the uncorrected stellar aberration due to the spacecraft velocity around the earth.

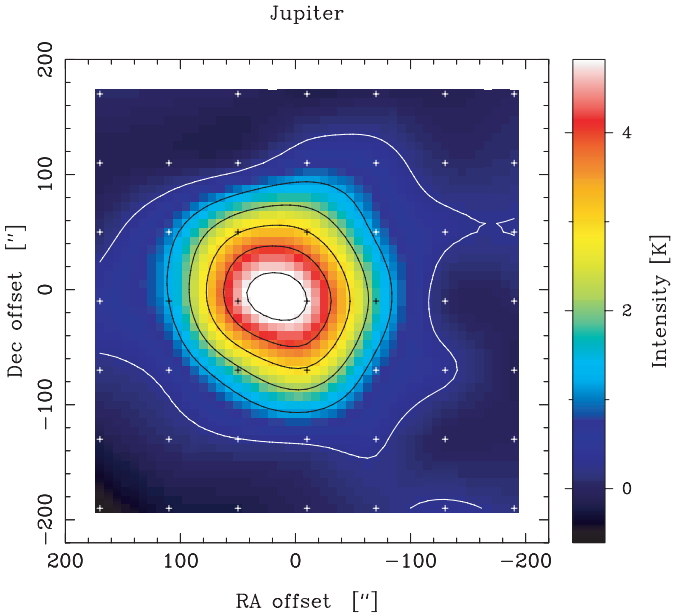

Fig. 7. Jupiter map at 557 GHz. The mapping, at 60″spacing, was performed in the position-switching mode, using a reference off at +1800″ in RA. The crosses denote map positions in our re-gridded map (best-fit after attitude reconstruction).

on October 6 and 20, 2002. The map is made up of 4 s integrations when the attitude reconstruction uncertainty was less than 7″. The observed HPBW is 140″ × 130″ and the peak antenna temperature is 5.35 K. The small but clearly visible elongation in RA may be ascribed to the larger attitude reconstruction inaccuracy in this direction, which is intrinsic to the configuration of the attitude control system (cf. Jakobsson et al. 2002a,b). The remaining RA offset of the emission peak will be discussed below. Using these values together with a Jupiter disc size of 33″ × 35″, an estimated Rayleigh-Jeans brightness of (124 ± 6) K at 557 GHz (Bergin et al. 2000; Moreno 1998) and a receiver image band rejection of 20 dB, we arrive at a HPBW of 126″ (2′.1) and a main beam efficiency of about (87 ± 6)%. Very similar values have been obtained from several earlier Jupiter maps in September 2001 and April 2002, assuring us that the antenna in-orbit characteristics are very close to our theoretical expectations, see Table 2.

Our main astronomical targets to observationally delineate the pointing stability and repeatability have been the thermal emission from Jupiter, the strong H_2O emission from several comets (Lecacheux et al. 2003), and the equally strong Orion KL H_2O outflow emission (Olofsson et al. 2003). Olofsson et al. find – by using the beam offsets observed towards Jupiter (see below) – that Odin in September 2001, April 2002 and October 2002 was able to place the Orion H_2O outflow centre to within a few arc seconds from the known centre of activity. These results indicate that the long-term pointing repeatability and the short-term attitude reconstruction accuracy are very good, probably within <10″. Figure 6 illustrate the pointing stability even after repeated interruptions by the Earth blocking the view of the star trackers.

Up to October 5, 2002 all Odin observations were performed with a known and stable antenna beam offset of about 30″ (counted from the assumed beam location in the star-tracker reference coordinate system). Our correction attempt, implemented on October 5, has reduced the current systematic instrumental offset error to be <10″ (cf. Fig. 7).

The receiver band around 572 GHz lost its phase lock soon after launch due to a broken harmonic mixer. New procedures to set the frequency were implemented and the receiver could be tuned over almost the original range although the frequency could not be set accurately and the frequency also drifts. One reason for the unlocked Gunn to drift is that the cavity is changing its size due to a change in temperature. During the 30 minutes of Earth occultation the frequency can be determined from atmospheric lines. By correlating temperature and frequency the frequency drift can be compensated for in the data processing. The Gunn is surprisingly stable even over an orbit (Larsson et al. 2003) and since the temperature sensor is mounted on the Gunn itself its reading is a very good indicator of relative frequency.

The 119 GHz receiver lost its phase lock October 14, 2001. The phase-lock was again recovered on March 9, 2002 using the spare Gunn source. The phase lock was again lost 3 months later. The cause for this failure is not known. But as with the 572 GHz receiver it is possible to use the lines in the Earth atmosphere to determine the observing frequency. One operational complication is that the drift has to be tracked by occasionally adjusting the frequency setting of the backend in order to keep it in the middle of the band.

During the first year both AC1 and AC2 lost one digitiser each, now understood to be an interface problem. They have

been reconfigured to avoid the bad segment but at some loss of performance. In the presently configured modes AC1 can have processed bandwidths of 700, 300 and 100 MHz and AC2 700, 300, 200 and 100 MHz depending on resolution. The AOS has had no anomalies except a stable modulation of Dicke switched spectra. It is removed by subtracting a reference spectrum and it is not present in position switched data.

We are utilising the fact that we have different backends and frontends to validate the observations and reach full agreement when observing the same spectral line with different frontends and backends. The processing of atmospheric data has also helped to verify that proper data reduction methods are used. We are now in a stable situation with well understood behaviour of both the spacecraft and the instruments and look forward to many years of fruitful observations. Odin is only limited by orbital decay and hardware failures with a still fully redundant spacecraft. We are planning to operate for at least 4 years which is 2 more than the design lifetime.

Acknowledgements. Many engineers and scientists from companies and institutes have worked very hard and contributed to the success of the Odin mission, sometimes inventing completely new methods to solve problems. We would here like to express our gratitude for having had the pleasure to work with you and wish that you are as proud of the excellent results being produced as we are.

References

Ala-Laurinaho, J., Hirvonen, T., Piironen, P., et al. 2001, IEEE Trans. Antennas Propag., 49, 1264

Bergin, E. A., Melnick, G. J., Stauffer, J. R., et al. 2000, ApJ, 539, L147

Emrich, A. 1996, in 30th ESLAB Symp., ESA-SP 388, 249

Emrich, A. 1997, Proc. ESA Symp.: The Far InfraRed and Submillimetre Universe, ESA SP-401, 361

Jakobsson, B., Nylund, M., Olsson, T., & Vinterhav, E. 2002, in 53rd International Space Congress, paper IAC-02-A.P.13

Jakobsson, B., Nylund, M., Olsson, T., Vandermarcq, O., & Vinterhav, E. 2002, in 53rd International Space Congress, paper IAC-02-A-4.01

Hjalmarsson, Å., Frisk, U. O., Olberg, M., et al., 2003, A&A, 402, L39

Larsson, B., Liseau, R., Bergman, P., et al. 2003, A&A, 402, L69

Lecacheux, A., Rosolen, C., & Michet, D. 1996, in 30th ESLAB Symp., ESA-SP 388, 253

Lecacheux, A., Rosolen, C., Michet, D., & Clerc, V. 1998, in Advanced Technology MMW, Radio and TeraHertz telescopes, ed. T. G. Phillips, Proc. SPIE, 3357, 519

Lecacheux, A., Biver, N., Crovisier, J., et al. 2003, A&A, 402, L55

Lehikoinen, P., Mallat, J., Piironen, P., et al. 1996, Int. J. Infrared Millimeter Waves, 17, 807

Lundin, S. 2002, in 53rd International Space Congress, paper IAC-02-IAA.11.4.04

Moldsvor, A., Kildal, P. S., & Frisk, U. O. 1994, Electrical design and tolerance study of the Odin telescope, in Nordic Antenna Conf. ANTENN-1994, Sundbyholm

Moreno, R. 1998, Doctoral thesis, Université Paris 6

Murtagh, D., Frisk, U. O., Merino, F., et al. 2002, Can. J. Phys., 80, 309

Olberg, M., Frisk, U. O., Lecacheux, A., et al. 2003, A&A, 402, L35

Olofsson, A. O. H., Olofsson, G., Hjalmarsson, Å., et al. 2003, A&A, 402, L47

Pagani, L., Olofsson, A. O. H., Bergman, P., et al. 2003, A&A, 402, L77

Piironen, P., Mallat, J., & Räisänen, A. V. 1998, IEEE Trans. Microwave Theor. Tech., 46, 1257

Ristorcelli, I., et al. 2003, Experimental Astronomy, in preparation

Sjöberg, F. 1996, in 47th International Astronautical Congress, paper IAF-96-I.1.11